HUMAN OCULOMOTOR CONTROL SIMULATION

Carter Compton Collins, Ph.D.
Smith-Kettlewell Institute and Department of Visual Sciences,
University of the Pacific, San Francisco, California, 94115

ABSTRACT

Techniques have been developed for monitoring human oculomotor innervation and unrestrained muscle forces during large eye movements. Results of these measurements have led to a better understanding of eye movement control strategies and an Interactive Simulation Language (ISL) model of the nonlinear peripheral oculomotor plant which duplicates both healthy and pathological eye movement performance.

This model matches physiological, nonlinear innervational and viscous properties of the oculomotor plant for large excursions, performing satisfactorily over the entire + or -50° range of eye movement. The model duplicates the family of muscle length-tension curves, traces the static locus and properly generates agonist and antagonist muscle forces observed in freely moving eyes during tracking and saccadic movements. It duplicates dynamic saccadic length-tension loops (the most critical test of model performance). It shows the effect of muscle shortening on forces during a saccade, and the initial force increase in a relaxing antagonist.

The model simulates both physiological and pathological human eye movement performance. For example, the tropia, overshoot, velocity, and eye movement magnitudes are each duplicated for lateral rectus palsy patients. In addition, the effects of internuclear ophthalmoplegia are likewise duplicated. This striking identity of model performance with known pathology has important bearing on the possible clinical uses of models which can be evaluated from patient measurements.

An individual patient clinical model may eventually be able to qualitatively and quantitatively aid the ophthalmologist in his diagnosis and choice of surgical treatment plan. Operation on the model would permit the surgeon to compare various amounts and types of strabismus surgery and choose an optimum approach from many model responses before going to the operating room.

INTRODUCTION

When a person is unable to direct both eyes at the same object his visual disorder is called strabismus. The clinical correction of strabismus generally involves surgically moving the point of attachment of one or both of the extraocular muscles to realign the eyes. However, some 20 to 40 percent of all strabismus surgical patients must return for reoperation[1]. Thus, there is clearly a need for a better understanding of the mechanical defects of strabismus and the surgery applied to overcome them.

METHODS

Computer simulation has become necessary for achieving a more complete and quantitative understanding of the many complex interrelationships involved in oculomotor control. Each anatomical element of the oculomotor plant must be separately represented since pathology and surgery affect each separately. Pathological ocular deviations are often significantly large, persisting to a great, but variable degree, over the entire range of ocular motility. Thus, a clinically useful model must be able to correctly simulate large eye movements embracing the performance of the grossly nonlinear oculomotor system over the complete range of plus or minus 50 degrees. The major nonlinearity is found in the relationship between the magnitude of innervation (the input control signal) and the position of the eye[2]. In addition, muscle viscosity varies as muscle tension and is a nonlinear function of eye movement velocity.

The techniques for measurement of these anatomical and physiological entities have been described elsewhere[3,4] and hence are only briefly outlined here. First, the muscle innervation, or input control signal, $\emptyset$, has been measured utilizing a specially developed multiple microelectrode technique for statistically sampling the simultaneous activity of up to 50 widely spaced, single motor units in a human oculorotary muscle during natural eye movements[3]. This is the equivalent of sampling the message on the oculomotor nerve as sent from the brain to the eye muscle. By this means we have found that the brain strategy utilizes a nonlinear (square-law) pattern of input innervation to control the position of eye fixation. Next, to measure *in situ* muscle tension forces, T, under the natural conditions existing during unrestrained eye movements it was necessary to develop a miniature, high-performance, implantable recording strain gauge which has been separately described along with the observed patterns of human eye muscle forces[4]. The elasticity, K, and viscosity, B, of the oculorotary muscles and passive globe (eyeball) restraining tissues have also been measured[5]. Eye position, θ, is measured conventionally, either photoelectrically[6] or by means of electro-oculography[7].

A model based on these new human physiological findings has been evolved over the past few years and an analog computer simulation[2] has now been adapted to Interactive Simulation Language (ISL) for more powerful, extensive and flexible basic and clinical applications. This model of the oculomotor plant and the differential equations describing eye movements are shown in Fig. 1. The model reflects our physiological findings that each eye muscle pair functions anatomically in a reciprocally innervated, class A, "push-pull" mode which compensates for (i.e., linearizes) the square law input innervation. This results in a linear muscle force *difference* acting on the

predominantly linear globe restraining elasticity. The end result is that the eye movement system appears to be linear when observed from the outside. However, you are aware of the more than linear effort required to hold your eyes at the extreme gaze position of 50° left or right.

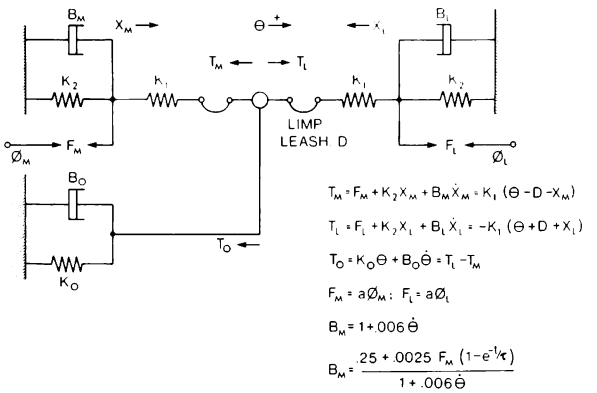

Fig. 1 - Diagram of the mechanical model of the human oculomotor plant and its differential equations of motion.

The physiologically measured input controls for this oculomotor plant model are represented in Fig. 2 as the static levels of innervation to the agonist and antagonist eye muscles, ϕ_M and ϕ_L. This transfer function relating the voluntary or desired eye position, Ψ, to the level of static innervation, ϕ, is the result of the strategy chosen by the brain to control the steady-state or fixation position of the eyes.

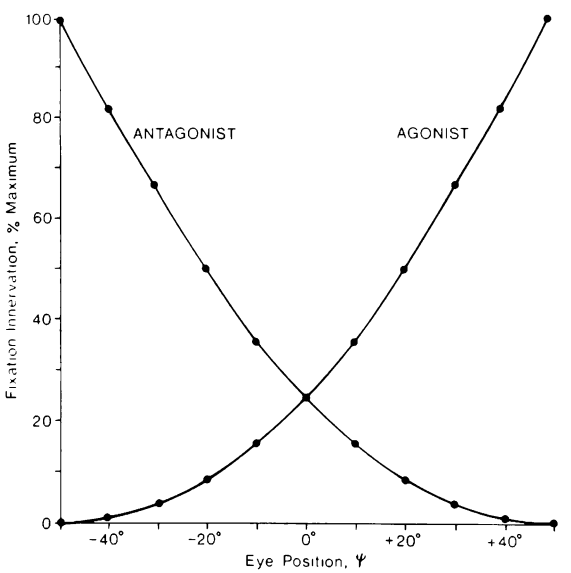

Fig. 2 - Steady-state input control signals (agonist and antagonist eye muscle innervation) as a function of eye position.

Superimposed upon this steady-state innervation are the transient control signals responsible for dynamic eye movements. The fastest eye movements are called saccades. These are quick, stepwise, coordinated movements of the eyes which are controlled by intricate, pre-programmed calculations of the central nervous system and result in remarkably accurate and rapid, precisely controlled flicking of the direction of gaze from one point to another. Figure 3 shows the magnitude and shape of the transient oculomotor control signals which produce saccades. These data have been hand averaged to remove the usual biological noise. Note a characteristic 10 msec. rise time to peak activity which is maintained for approximately one-half of the saccadic duration and falls with a time constant having a value of approximately one-fifth of the saccadic duration. The exact nature of the instantaneous value of this eye movement control signal is important in determining the transient time course of eye movements during saccades where large, inconstant and nonlinear viscous forces predominantly dictate movement.

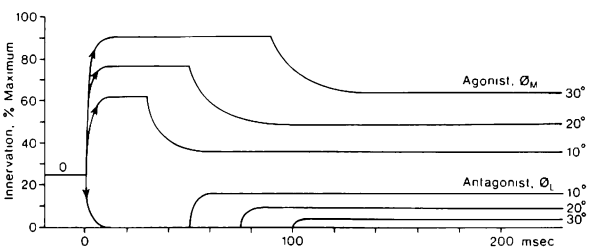

Fig. 3 - The time-varying pattern of the dynamic control signals of the eye muscles. These signals are superimposed on the steady-state levels to produce fast eye movements called saccades.

These physiologically measured, complex human eye movement control signals are used as inputs to drive the ISL model of the human oculomotor plant shown in the block diagram, Fig. 4. The left hand portion of the diagram performs the function of the central nervous system in generating these complex input control signals. In the upper left, Ψ_0 represents the initial desired voluntary eye position (for example, straight ahead, the so-called primary position). Ψ_1 then represents the desired new position of the eyes in degrees. The summer and multiplier in the upper and lower left portions of the diagram generate the steady-state innervation functions of Fig. 2. The left central elements of this model generate the transient components of the saccadic eye movement control signal which are added to the static components resulting in the complete eye movement control signals ϕ_M and ϕ_L.

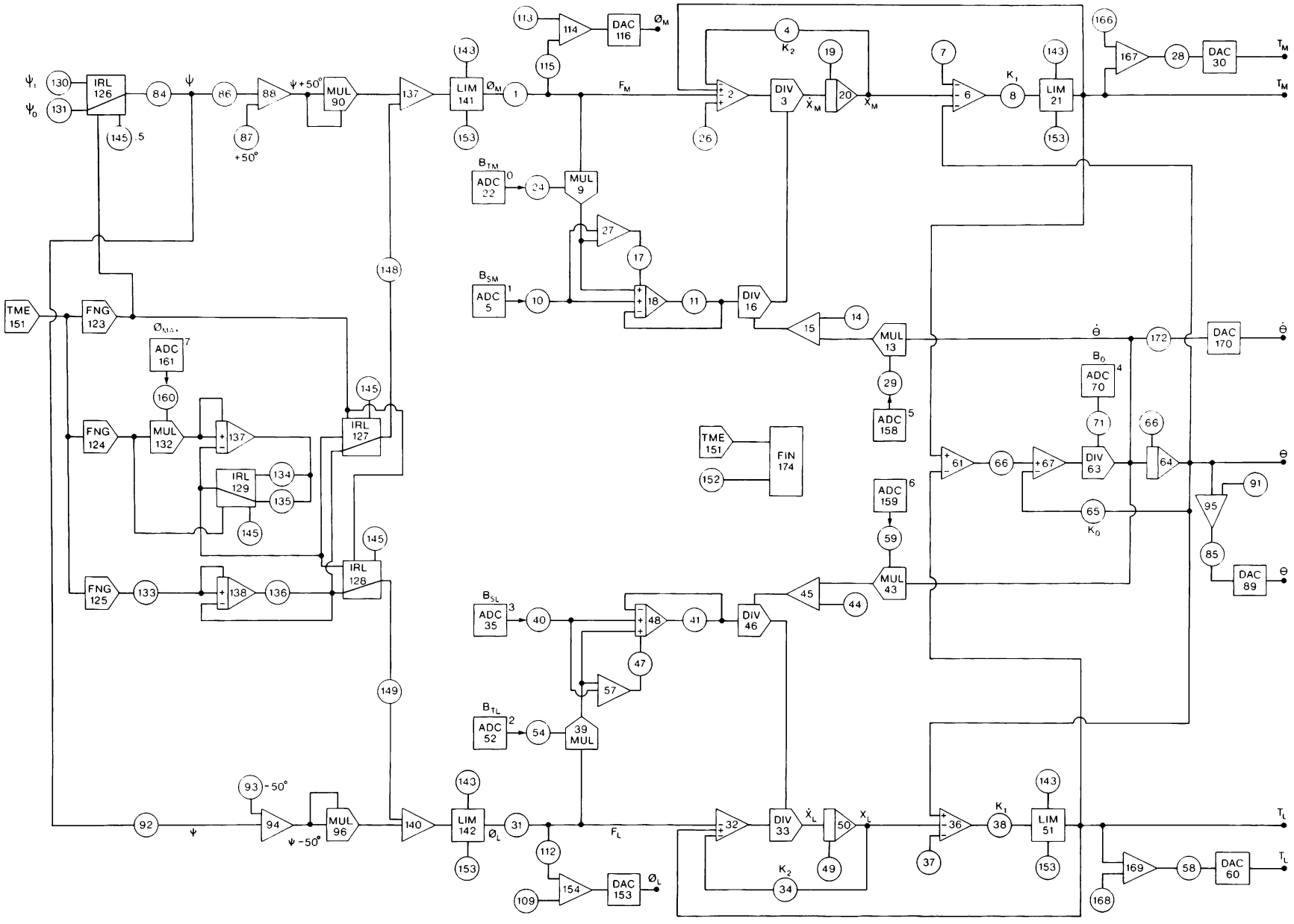

FIG. 4 - BLOCK DIAGRAM OF THE OCULOMOTOR PLANT

Fig. 5 - ISL listing of the oculomotor plant simulation programmed for 0 to 20° right saccade of left eye.

```
HUMAN OCULOMOTOR CONTROL SIMULATION

0   CON   0                    = 5.000E-3      0
1   POT   141,  1.500E-2       = 3.749E 1      1
2   ADD   -1, -4, 21, 26       = 1.107E 0      2
3   DIV   2, 16                = 2.844E 0      3
4   POT   20,  1.200E 0        =-2.931E 1      4
5   ADC   1                    = 1.113E 0      5
6   ADD   -7, -20, -64         = 3.713E 0      6
7   CON   7                    = 2.000E 1      7
8   POT   6,  2.500E 0         = 9.281E 0      8
9   MUL   1, 24                = 1.062E-1      9
10  POT   5,  2.500E-1         = 2.783E-1      10
11  POT   18,  3.000E 1        = 3.838E-1      11
12  POT   3,  0.000E 0         = 0.000E 0      12
13  MUL   63, 29               =-1.397E-2      13
14  CON   14                   = 1.000E 0      14
15  ADD   13, 14               = 9.860E-1      15
16  DIV   163, 15              = 3.892E-1      16
17  POT   27,  1.000E-2        = 3.840E-3      17
18  INT   17, 9, 10, -11       = 1.280E-2      18
19  CON   19                   =-2.500E 1      19
20  INT   19, 3                =-2.442E 1      20
21  POT   8,  1.000E 0         = 9.281E 0      21
22  ADC   0                    = 1.133E-1      22
23  CON   23                   = 3.000E 2      23
24  POT   22,  2.500E-2        = 2.832E-3      24
25  POT   16,  1.000E 3        = 3.892E 2      25
26  POT   0,  0.000E 0         = 0.000E 0      26
27  ADD   9, 10                = 3.845E-1      27
28  POT   167,  9.000E-1       = 2.635E 1      28
29  POT   158,  2.500E-3       = 5.224E-3      29
30  DAC   28, 118, 64          = 0.328E-1      30
31  POT   142,  1.500E-2       = 3.750E 1      31
32  ADD   -31, -34, 51         =-1.071E 0      32
33  DIV   32, 46               =-2.804E 0      33
34  POT   50,  1.200E 0        =-2.745E 1      34
35  ADC   3                    = 1.088E 0      35
36  ADD   -37, -50, 64         = 3.593E 0      36
37  CON   37                   = 2.000E 1      37
38  POT   36,  2.500E 0        = 8.982E 0      38
39  MUL   31, 54               = 1.044E-1      39
40  POT   35,  2.500E-1        = 2.720E-1      40
41  POT   48,  3.000E 1        = 3.765E-1      41
42  POT   33,  0.000E 0        = 0.000E 0      42
43  MUL   63, 59               =-1.410E-2      43
44  CON   44                   = 1.000E 0      44
45  ADD   43, 44               = 9.859E-1      45
46  DIV   165, 45              = 3.818E-1      46
47  POT   57,  1.000E-2        = 3.763E-3      47
48  INT   47, 39, 40, -41      = 1.255E-2      48
49  CON   49                   =-2.500E 1      49
50  INT   49, 33               =-2.288E 1      50
51  POT   38,  1.000E 0        = 8.982E 0      51
52  ADC   2                    = 1.113E-1      52
53  CON   53                   = 3.000E 2      53
54  POT   52,  2.500E-2        = 2.783E-3      54
55  POT   46,  1.000E 3        = 3.818E 2      55
56  CON   56                   = 0.000E 0      56
57  ADD   39, 40               = 3.763E-1      57
58  POT   169,  9.000E-1       = 2.608E 1      58
59  POT   159,  2.500E-3       = 5.259E-3      59
60  DAC   58, 118, 64          = 0.326E-1      60
61  ADD   21, -51              = 2.993E-1      61
62  CON   62                   = 0.000E 0      62
63  DIV   67, 71               =-2.662E 0      63
64  INT   62, 63               = 7.097E-1      64
65  POT   64,  5.000E-1        = 3.549E-1      65
66  POT   61,  1.000E 0        = 2.993E-1      66
67  ADD   66, -65              =-5.554E-2      67
68  POT   67,  5.000E 0        =-2.777E-1      68
69  POT   64,  5.000E 0        = 3.549E 0      69
70  ADC   4                    = 8.379E-1      70
71  POT   70,  2.500E-2        = 2.095E-2      71
72  CON   72                   = 0.000E 0      72
73  CON   73                   = 0.000E 0      73
74  CON   74                   = 0.000E 0      74
75  CON   75                   = 0.000E 0      75
76  CON   76                   = 0.000E 0      76
77  CON   77                   = 0.000E 0      77
78  CON   78                   = 0.000E 0      78
79  CON   79                   = 0.000E 0      79
80  POT   122,  1.000E 0       = 0.000E 0      80
81  POT   80,  1.000E 0        = 0.000E 0      81
82  CON   82                   = 0.000E 0      82
83  INT   82, 81, -84          =-3.161E 2      83
84  POT   126,  1.000E 0       = 0.000E 0      84
85  POT   95,  8.400E-1        = 9.000E 0      85
86  POT   84,  1.000E 0        = 0.000E 0      86
87  CON   87                   = 5.000E 1      87
88  ADD   86, 87               = 5.000E 1      88
89  DAC   85, 119, 64          = 0.112E-1      89
90  MUL   88, 88               = 2.500E 3      90
91  CON   91                   = 1.000E 1      91
92  POT   84,  1.000E 0        = 0.000E 0      92
93  CON   93                   = 5.000E 1      93
94  ADD   92, -93              =-5.000E 1      94
95  ADD   64, 91               = 1.071E 1      95
96  MUL   94, 94               = 2.500E 3      96
97  CON   97                   =-0.000E 0      97
98  CON   98                   = 1.000E-2      98
99  CON   99                   = 0.000E 0      99
100 POT   103,  1.500E-2       = 1.960E 59     100
101 CON   101                  =-5.000E 1      101
102 ADD   100, 101             = 1.960E 59     102
103 TDL   106, 104, 105        = 1.307E 61     103
104 CON   104                  = 1.000E 0      104
105 CON   105                  = 2.500E 2      105
106 POT   151,  1.000E 0       = 1.500E 0      106
107 TDL   110, 108, 109        = 2.774E 63     107
108 CON   108                  = 0.000E 0      108
109 CON   109                  = 5.000E 1      109
110 CON   110                  = 0.000E 0      110
111 CON   111                  = 0.000E 0      111
112 POT   31,  1.000E-1        = 3.750E 0      112
113 CON   113                  = 5.000E 1      113
114 ADD   113, 115             = 5.375E 1      114
115 POT   1,  1.000E-1         = 3.749E 0      115
116 DAC   114, 118, 64         = 0.671E-1      116
117 CON   117                  = 1.000E 0      117
118 CON   118                  = 1.000E 2      118
119 CON   119                  = 1.000E 2      119
120 CON   120                  = 0.000E 0      120
121 CON   121                  = 0.000E 0      121
122 CON   122                  = 0.000E 0      122
123 FNG   151                  = 0.000E 0      123
        0.000E 0     0.000E 0
        4.900E-2     0.000E 0
        5.000E-2     1.000E 0
        5.000E-1     1.000E 0
        5.010E-1     0.000E 0
        1.000E 0     0.000E 0
        1.000E 1     0.000E 0
124 FNG   151                  = 0.000E 0      124
        0.000E 0     0.000E 0
        4.900E-2     0.000E 0
        5.000E-2     1.000E 0
        1.000E-1     1.000E 0
        1.010E-1     0.000E 0
        1.000E 0     0.000E 0
        1.000E 1     0.000E 0
125 FNG   151                  = 0.000E 0      125
        0.000E 0     0.000E 0
        4.900E-2     0.000E 0
        5.000E-2    -1.000E 0
        1.250E-1    -1.000E 0
        1.260E-1     0.000E 0
        1.000E 0     0.000E 0
        1.000E 1     0.000E 0
126 IRL   123, 145, 130, 131       = 0.000E 0
127 IRL   123, 145, 137, 136       =-3.773E-204
128 IRL   123, 145, 136, 129       = 7.634E-32
129 IRL   124, 145, 134, 135       = 6.773E-32
130 CON   130                  = 2.000E 1      130
131 CON   131                  = 0.000E 0      131
132 MUL   124, 160             = 0.000E 0      132
133 POT   125,  1.200E 3       = 0.000E 0      133
134 POT   137,  2.500E 2       = 3.005E-31     134
135 POT   137,  5.000E 1       = 6.011E-32     135
136 POT   138,  2.500E 2       =-1.886E-204    136
137 INT   132, 132, -129       = 1.067E-33     137
138 INT   133, 133, -136       =-3.773E-207    138
```

```
139 ADD   90, 148          = 2.500E 3     139
140 ADD   96, 149          = 2.500E 3     140
141 LIM   143, 153, 139    = 2.500E 3     141
142 LIM   143, 153, 140    = 2.500E 3     142
143 CON   143              = 1.000E 5     143
144 DAC   154, 118, 64     = 0.671E-1     144
145 CON   145              = 5.000E-1     145
146 IRL   123, 145, 132, 147       = 0.000E 0
147 POT   124,  5.000E 1   = 0.000E 0     147
148 POT   127,  2.000E 0   =-7.546E-204     148
149 POT   128,  1.000E 0   = 7.634E-32     149
150 CON   150              = 0.000E 0     150
151 TME   151              = 1.502E 0     151
152 CON   152              = 1.500E 0     152
153 CON   153              = 0.000E 0     153
154 ADD   109, 112         = 5.375E 1     154
155 CON   155              = 0.000E 0     155
156 CON   156              = 0.000E 0     156
157 CON   157              = 1.000E 3     157
158 ADC   5                = 2.090E 0     158
159 ADC   6                = 2.105E 0     159
160 POT   161,  1.875E 5   = 5.830E 5     160
161 ADC   7                = 3.123E 0     161
162 INT   11, 11, -163     = 1.279E-2     162
163 POT   162,  3.000E 1   = 3.838E-1     163
164 INT   41, 41, -165     = 1.255E-2     164
165 POT   164,  3.000E 1   = 3.765E-1     165
166 CON   166              = 2.000E 1     166
167 ADD   21, 166          = 2.928E 1     167
168 CON   168              = 2.000E 1     168
169 ADD   51, 168          = 2.898E 1     169
170 DAC   172, 118, 64     = 0.000E 0     170
171 DAC   151, 117, 128    = 1.249E-1     171
172 POT   63,  2.500E-2    =-6.654E-2     172
173 DAC   143, 143, 64     = 1.249E-1     173
174 FIN   151, 152         = 0.000E 0     174
175 END   0                =-7.831E 1227     175
```

The upper and lower right elements of the model represent the medial and lateral rectus respectively. The contractile element consists of two dividers, a multiplier and an integrator to represent respectively the nonlinear muscle viscosity as a function of developed tension, eye movement velocity and the temporal dynamics of the contractile element. The series elastic element, K1 of each muscle is on the right of the collection of muscle elements. The muscle outputs consist of tendon tensions, T_M and T_L.

These muscle tensions are algebraically added and applied to the globe dynamics, K_O and B_O, in the right central portion of the model. The resulting output is seen as eye position, θ, and eye movement velocity, $\dot{\theta}$.

Figure 5 is an ISL listing of the oculomotor plant model described here.

RESULTS

Figure 6 shows the model output performance characteristics on the length-tension plane as reproduced directly from a storage oscilloscope. Figure 7 is a hand-traced rendition of these curves labeled for greater clarity. These data agree quite well with recorded physiological measurements on human oculorotary muscle patients. In fact, Fig. 7 can serve as a summary of the measured physiological output of the normal human oculomotor plant[2] showing both the steady-state and dynamic performance of this system on the length-tension plane. Muscle length increases to the right and is shown in terms of eye position.

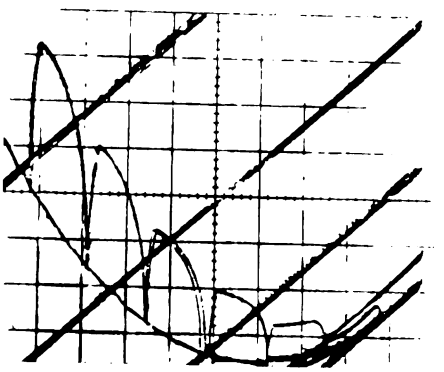

Fig. 6 - Static and dynamic performances of the model on the length-tension plane taken directly from a storage oscilloscope output.

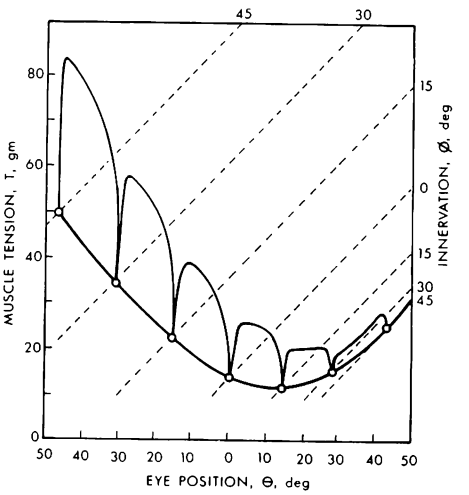

Fig. 7 - Labeled drawing of the model outputs of Fig. 6 showing length-tension characteristics of a muscle, the static locus and dynamic saccadic loops.

Right gaze is to the right on the diagram. The dashed lines in this figure represent the family of length-tension curves of the left lateral rectus muscle as a function of various degrees of fixed innervation shown as the parameter on the right hand ordinate. Zero indicates an innervation for zero degrees, or straight ahead; progressing upward the numbers represent increasing innervation to the labeled positions of gaze into the muscle's field of action, in this case, left gaze. Downward, innervation is decreasing to the labeled positions of right gaze out of the muscle's field of action. Note that these curves are not evenly spaced reflecting the nonlinearity of input innervation.

The heavy curved line intersecting the small circles at the bottom of the diagram indicates the measured tensions utilized by the oculomotor system to hold the eye at any degree of eccentric gaze. We call this curve the static locus of fixation tensions. Tensions recorded during smooth following movements of the eyes fall on or slightly above this static locus.

Typical dynamic length-tension loops for 15° fast saccadic movements of the eyes produced by the agonist (active) muscle are shown in Figs. 6 and 7 as counterclockwise-traced force pulses extending between the open circles on the static locus. These circles represent the starting (right) and finishing (left) points of saccadic eye position. [A typical dynamic length-tension loop for the antagonist (relaxing) muscle would be shown as a much smaller, flattened clockwise path moving to the right between the initial (left) and final (right) positions of the eye.] The tops of the saccadic force peaks in Fig. 7 define an upper curved line which represents the maximum forces recorded during any eye movement. The area between this upper curve and the static locus we call the operational envelope. This operational envelope defines the normal ranges of tensions for horizontal eye movements as measured during the waking state. The operational envelope of normal eye movement forces measured at the tendon of the muscle is determined by neuromuscular control, the innervational strategy of the central nervous system operating on the mechanical viscoelastic characteristics of the muscles and globe. The combination of these factors restricts normal muscle activity to a mere 20 percent of the area of the length-tension diagram. All areas on the length-tension diagram outside the operational envelope are forbidden regions during normal eye movements. Only during abnormal or pathological conditions do the muscle forces leave the operational envelope area of the length-tension diagram. Thus, the operational envelope has clinical significance relating to diagnosis utilizing forced duction or other techniques.

In the model of Figs. 1 and 4, the contractile element force consists of three components: the developed force, F, due to innervation, ϕ ; the force-velocity relationship of the muscle, or viscosity, B; and the force due to the parallel elastic element, K_2, contributing to the length-tension characteristic of muscle. The sum of these three forces is equal to the force measured at the muscle tendon. However, any one component of this contractile element force cannot be uniquely determined at the tendon because of the isolating series elastic element, K_1.

Figure 8 is a time based record of the performance of the model left eye in response to a zero to 20-degree right saccadic input innervation, ϕ_M of the medial rectus muscle shown on the top channel of the oscillographic record. The next lower record shows the innervation, ϕ_L of the antagonist lateral rectus muscle which was reciprocally innervated, in this case turned completely off during the saccade in accord with the quantitative results of physiological measurements of innervation.

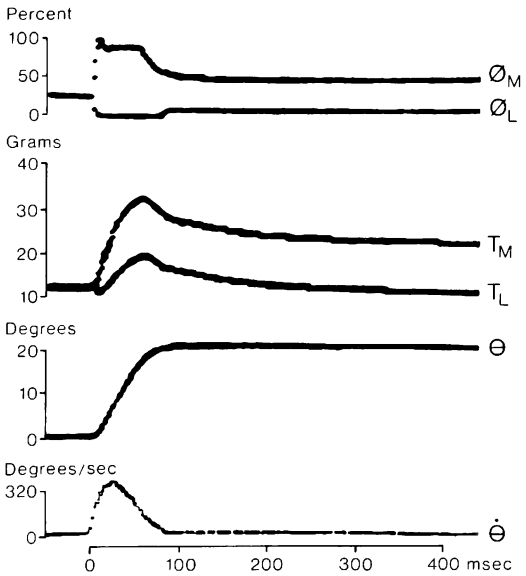

Fig. 8 - Dynamic performance of the model as a function of time in response to the reciprocal innervation, ϕ_M and ϕ_L (top traces) for a zero to 20° right saccade of the left eye. The middle traces are muscle tensions, T_M and T_L, and the lower traces are eye position, θ, and velocity, $\dot{\theta}$.

The next two records are those of model-derived muscle tensions, T_M and T_L, of the medial and lateral rectus muscles respectively. The agonist medial rectus muscle force is seen to be greater, peaking in about 50 msec and then slowly decaying to its steady-state fixation or holding value. Just below it, the lateral rectus muscle tension is also seen to increase before decreasing to its final steady-state value. This increase was unexpected since the lateral rectus muscle innervation drops to zero during the saccade, and separate isometric measurements of this antagonist muscle force have shown that the muscle force drops below baseline tensions. The reason for the muscle force increase is that this antagonist muscle is stretched by the agonist muscle at a rate which causes the antagonist muscle viscous forces to increase more rapidly and with greater magnitude than the force decrease due to the drop in innervation. Both the agonist and antagonist model muscle forces faithfully reproduce the patterns and magnitude of forces as measured by our "C" gauges implanted in human oculorotary muscles during strabismus surgery(4).

The next lower record represents the resultant eye movement, θ, which again truly represents the pattern of eye movement seen in normal human subjects. Finally, the lowest record shows the eye movement velocity, $\dot{\theta}$, which again is a sensitive test of model performance. This velocity profile agrees quite well with measured human eye movement data and again illustrates the realistic performance of this oculomotor plant simulation.

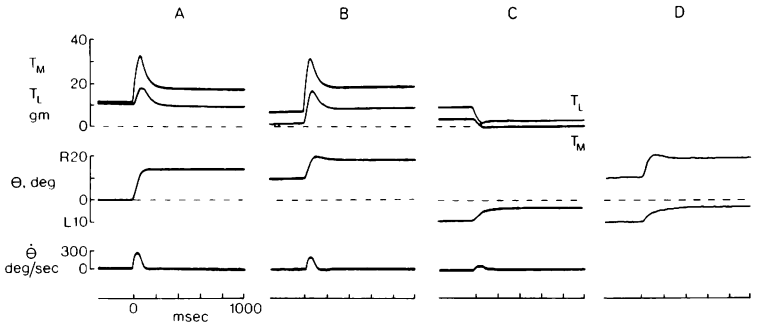

Fig. 9A - Oculomotor model simulation of a normal left eye.
9B - Simulation of a pathological eye movement with a paralyzed antagonist left lateral rectus muscle.
9C - Simulated pathological eye movement with a paralyzed agonist left medial rectus muscle.
9D - Actual patient records of a lateral rectus palsy patient. Note how closely these are duplicated by the model.

Figure 9 compares pathological oculomotor performance with the normal performance record of Fig. 8. Figure 9A is an oculomotor simulation of a normal left eye during a 0 to 15-degree right saccade. At the top are the unrestricted medial and lateral muscle tensions, T_M and T_L, shown on the same scale to illustrate comparative performance. The next lower trace shows eye position, θ. The bottom trace indicates velocity, $\dot{\theta}$.

Figure 9B shows the model simulation of a pathological left eye during a 15° right saccade with a paralyzed antagonist left lateral rectus muscle. Note the 10° right esotropia (inward misalignment), 3° saccadic overshoot, 150° per second velocity (about half normal), and 8° final eye movement instead of the normal 15°.

Figure 9C shows the model simulation of a pathological left eye movement during a 15° right saccade with a paralyzed agonist left medial rectus muscle. Note the 10° left exotropia (outward misalignment), 500 msec saccadic duration, 60° per second velocity, and 7° final eye movement.

Figure 9D presents eye movement records of a lateral rectus palsy patient. The top record with a palsied antagonist shows the tropia, overshoot, velocity, and size of eye movement which are duplicated by the model in Fig. 9B. The bottom trace is a patient record of movement with a palsied muscle acting as agonist. Note the model duplicates this pathological eye movement in Fig. 9C.

DISCUSSION

It can be seen that the model simulates both physiological and pathological human eye movement performance. This striking identity of model performance with known pathology has important bearing on the possible clinical uses of models which can be evaluated from patient measurements. By making simple clinical office measurements with a strain gauge forceps it appears to be possible to evaluate the various model elements of the patient's oculomotor plant in the surgeon's office. Calibrated forceps measurements[8] of isometric forces during contralateral eye fixations can determine neuromuscular functional imbalances; and contractures or mechanical restrictions may be quantitatively determined in the office with position monitored forceps measurements of ocular length-tension characteristics.

An individual patient clinical model thus resulting may be able to quantitatively and qualitatively aid the ophthalmologist in his diagnosis and choice of surgical treatment plan. An interactive graphic CRT display now under development in our laboratories would provide immediate feedback indicating the results of various combinations of simple surgical techniques on oculomotor performance and alignment. For example, the effects of surgery on comitance (relative alignment of the eyes) could be instantly and directly displayed in graphical form. Simulated surgery on the model would permit an ophthalmologist to explore various types and amounts of corrective surgery. He would then have the choice of pursuing a conventional plan or of considering a different surgical approach suggested by newly derived computer data based on quantitative measurements of the patient before going to surgery.

ACKNOWLEDGEMENTS

The author gratefully acknowledges the collaboration of Dr. Alan Scott in collecting the patient data from which the reported results have been derived. The assistance of Mr. David O'Meara in muscle force studies is also greatly appreciated. This investigation was supported by NIH research grants Nos. PO1 EY-01186, PO1 EY-00299 and PO1 EY-00498 from the National Eye Institute; No. SO1 RR-05566 from the Division of Research Resources, and the Smith-Kettlewell Eye Research Foundation.

REFERENCES

(1) Costenbader, F. D., Infantile esotropia. Trans. Amer. ophthal. Soc. 59:397-429, 1961.

(2) Collins, C. C., The human oculomotor control system, In, Basic Mechanisms of Ocular Motility and Their Clinical Implications, G. Lennerstrand, P. Bach-y-Rita (Eds.), Oxford, England, Pergamon Press, Ltd., 1975, pp 145-180.

(3) Collins, C. C. and A. B. Scott, The eye movement control signal, Proc. Second Bioengineering Conference, Milan, Italy, 1973.

(4) Collins, C. C., D. O'Meara and A. B. Scott, Muscle tension during unrestrained human eye movements. J. Physiol. 245:351-369, 1975.

(5) Collins, C. C., Orbital mechanics. In, The Control of Eye Movements, P. Bach-y-Rita and C. C. Collins (Eds.), New York, Academic Press, 1971, pp. 283-325.

(6) Stark, L. and A. Sandberg, A simple instrument for measuring eye movements, Quart. Prog. Rept., Research Laboratory of Electronics, MIT 62:286-270, 1961.

(7) Shackel, B. Review of the past and present in oculography. Proc. Second International Conf. on Medical Electronics, Paris, France, Iliffe and Sons, London, 1960.

(8) Scott, A. B., C. C. Collins and D. O'Meara, A forceps to measure strabismus forces. Arch. Ophthal. 88:330-333, 1972.